



Total Ionizing Dose Effect Study on Radiation-Hard Power MOSFET Device

P. Kerber (pkerber@sandia.gov), K. M. Leeson, X. Gao, L. C. Musson, P. M. Campbell, M. L. McLain, B. S. Paskaleva, and A. Mar
Sandia National Laboratories, Albuquerque NM 87185

Abstract

TID study on radiation-hardened power MOSFET was carried out as a function of total dose, dose-rate, device state, and annealing time. Experimental data was correlated to interface trap and oxide charge density using TCAD simulations.

Introduction

- Commercially available, radiation-hardened, planar, vertical double-diffused power MOSFETs continue to be used pervasively for space and strategic applications. [1]
- Despite the engineered radiation hardness, these devices are susceptible to TID effects. The primary degradation mode due to ionizing radiation exposure is a shift in the threshold voltage (ΔV_T).
- This work examines and compares post-irradiation test data and simulation results for transistors exhibiting significant defect growth and annealing effects due to TID.

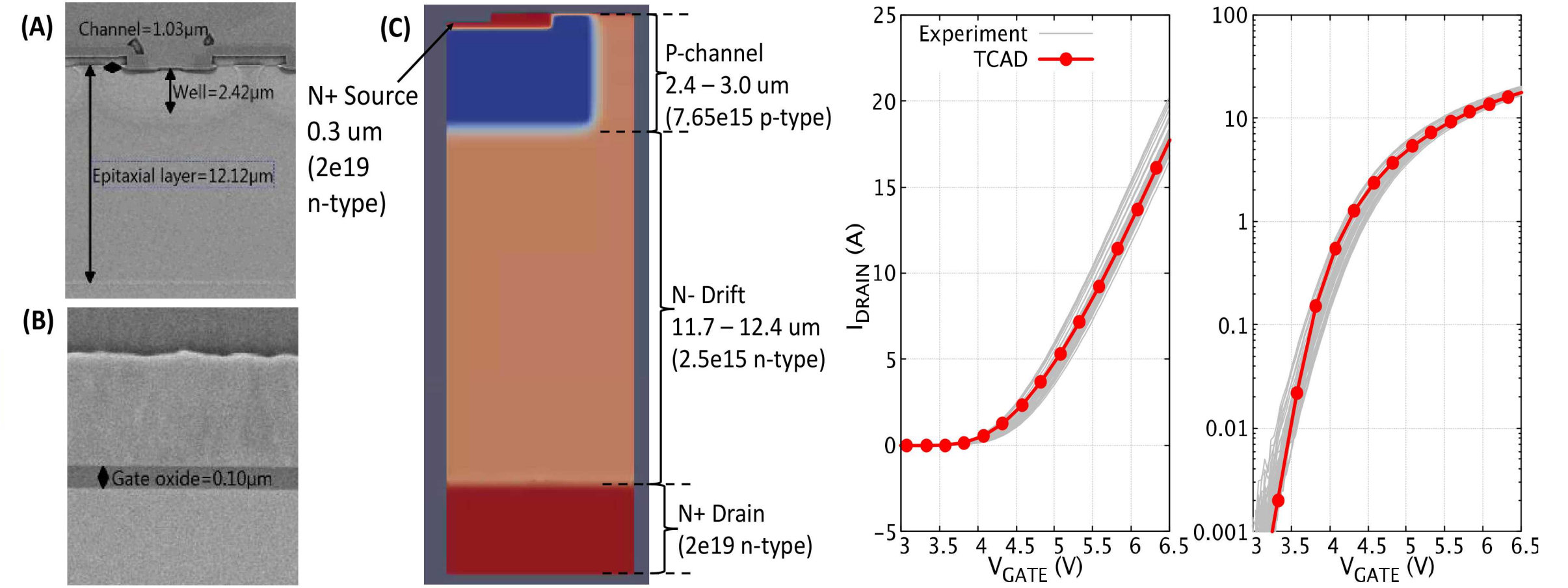


Fig. 1 Cross-sectional SEM of NMOS power MOSFET device showing (A) junction depths, channel length and (B) gate oxide thickness. (C) Junction doping and placement used for TCAD calibration.

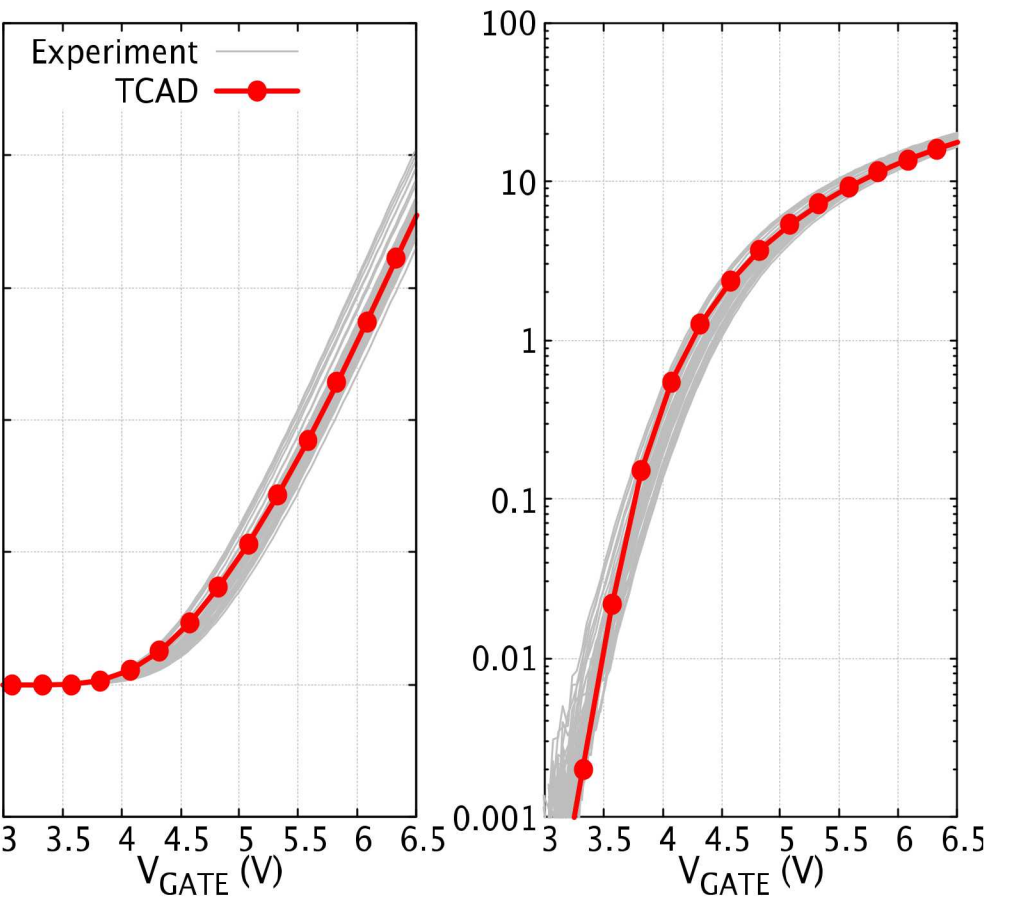


Fig. 2 I_D - V_{GS} plot showing match between experimental data (gray lines) and TCAD simulation (red) on linear (left panel) and semi-log (right panel) scales.

Experimental Details

Radiation Sources & Dosimetry:

- GIF: Co-60 source at 250 rad(Si)/s with total measurement uncertainty < 10%
- LINAC: Nominal electron energy 20 MeV; dose-rate 1.1×10^6 and 1.1×10^7 rad(Si)/s with pulse width ranging from 9 μs – 36 μs. Measurement accuracy $\pm 10\%$

Devices & Measurement:

- International Rectifier's NMOS power MOSFETs IRHN53130 with "moderate" TID hardness of 300 krad (Si).
- GIF: $V_{GS} = -6V$ (off-state), $+6V$ (on-state), and $0V$ with $V_{DS} = 28V$. Samples accumulated TID from 100 krad to 1Mrad with intermittent I-V measurements
- LINAC: $V_{GS} = -6V$ (off-state), $+6V$ (on-state) with $V_{DS} = 28V$. Individual devices exposed to 100, 200, 500, and 1000 krad(Si). [No dose accumulation as in GIF case.]
- Pre- and post-irradiation I_D - V_{GS} and I_D - V_D sweeps using Keysight B1505A parametric analyzer

Simulation Set Up

- 2D TCAD simulations of power MOSFET devices were performed using CHARON.
- A normal-environment device calibration was performed by modifying junction doping and its placement, SD parasitic resistance, mobility, and saturation velocity parameters

Results & Discussion

Time-Dependent Response:

- ΔV_T shows $\text{Log}(t)$ recovery rate irrespective of V_G and dose-rate [2,3]
- Annealing rate [slope of ΔV_T versus $\text{Log}(t)$] is lower for $-V_{GS}$ condition than for $+V_{GS}$ condition explained by tunneling of electrons from silicon into the oxide traps. [4]
- For $-V_{GS}$, charge centroid near gate; for $+V_{GS}$ charge centroid near silicon channel; Capture cross-section decreases exponentially with distance from the channel interface [5]

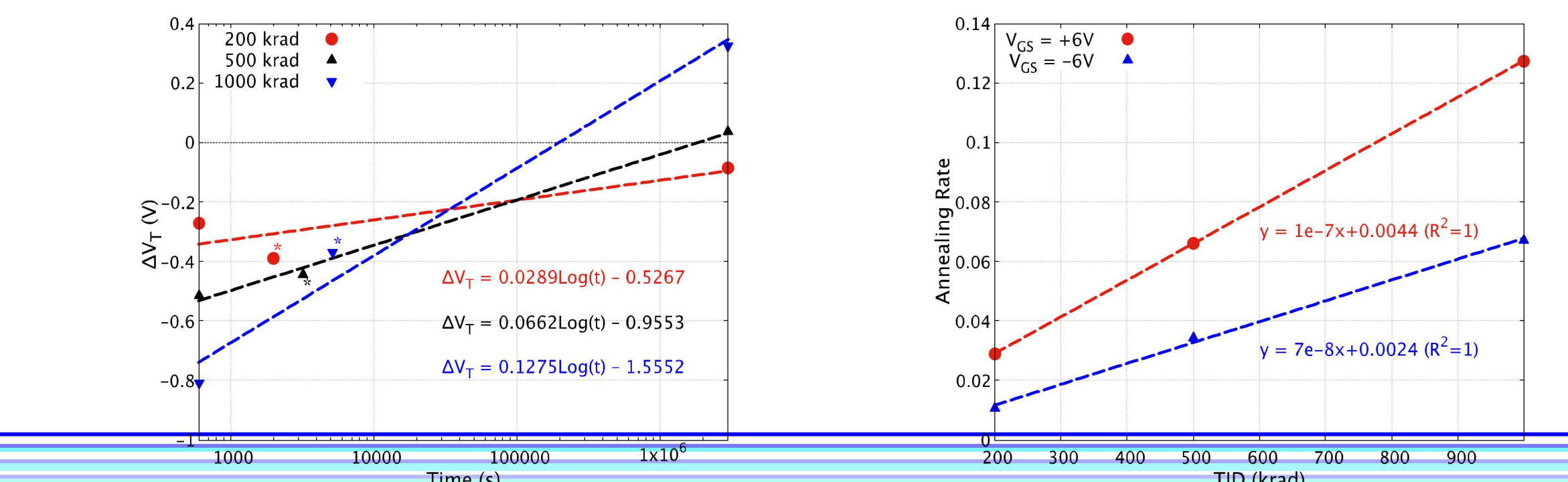


Fig. 3 (Left) ΔV_T as a function of post-irradiation annealing time; devices were irradiated at $V_{GS} = 6V$. (Right) annealing rate as a function of TID for $V_{GS} = +6$ and $-6V$.

Threshold Voltage v/s TID Response:

- For a given V_{GS} , max. ΔV_T for GIF devices is half compared to that for LINAC devices. This is due to longer exposure time (low dose-rate) and longer measurement delay at GIF facility leading to longer sample annealing time.
- GIF data as a function of TID reveals larger ΔV_T for $+V_{GS}$ conditions relative to the $-V_{GS}$ condition. This is related to oxide charge centroid location (Fig. 5, left panel).

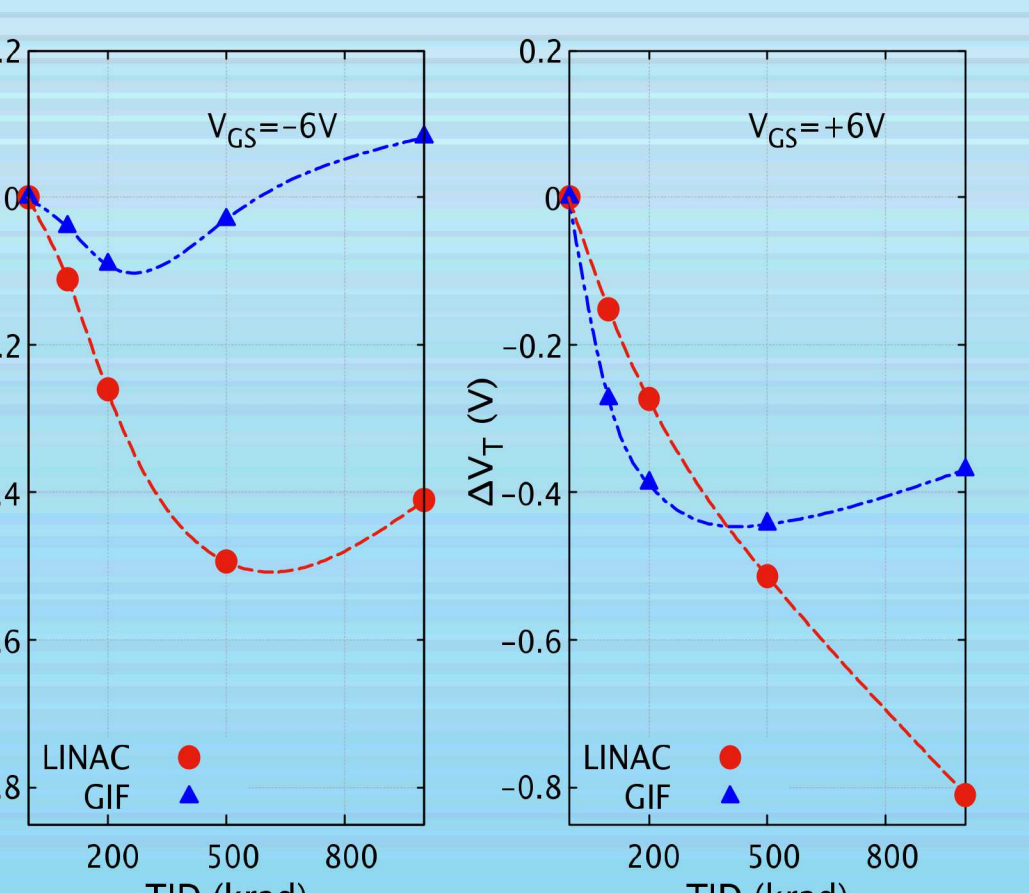


Fig. 4 ΔV_T vs. TID for LINAC and GIF samples with $V_{GS} = -6V$ (left panel) and $V_{GS} = +6V$ (right panel) during irradiation.

- GIF $V_{GS} = -6V$ condition at 1 Mrad shows V_T rebound of about 100 mV indicative of buildup of radiation-induced acceptor-type trap states at the Si/SiO₂ interface.
- TCAD results of ΔV_T as a function of interface trap density (Fig. 5, right panel) indicate an interface trap density of $3-4 \times 10^{10}/\text{cm}^2$ for 100mV ΔV_T . [6]
- ΔV_T for LINAC samples (red curves, Fig. 4) is nearly the same up to 500 krad TID for both V_{GS} cases and needs further investigation.

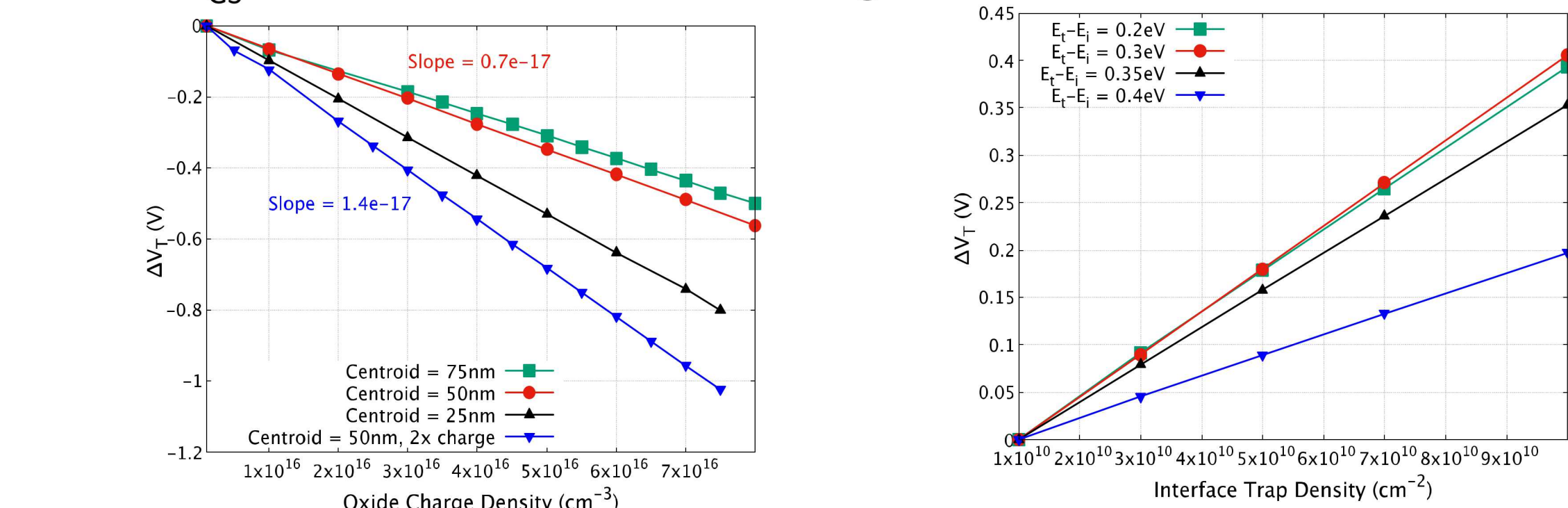


Fig. 5 TCAD results for ΔV_T as a function of positive bulk oxide charge density for different charge centroid locations (left) and interface trap density for various energy locations in the band-gap (right).

$V_{GS} = 0V$ During Irradiation at GIF:

- V_T recovery slightly above 200 krad and a strong rebound for higher TID levels. ΔV_T rebound of 300 mV at 500 krad suggests an interface trap density of $\sim 8 \times 10^{10}/\text{cm}^2$ (Fig. 5)
- At the 1 Mrad condition, a ~ 350 mV positive shift in I_D - V_{GS} curve attributable to negative bulk oxide [7] charge and accounts for nearly all of the rebound effect w.r.t the 500 krad sample

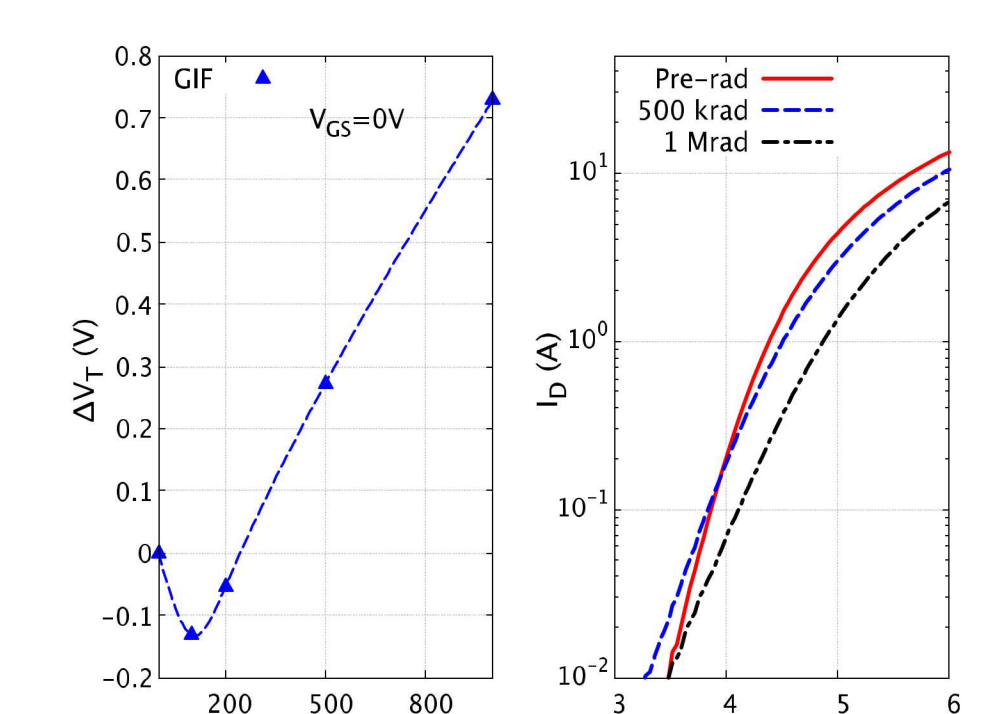


Fig. 6 ΔV_T versus TID for $V_{GS} = 0V$ sample irradiated at GIF (left panel), and corresponding I_D - V_{GS} measurements (right panel).

Conclusions & Future Work

- RT annealing indicate ΔV_T recovery rate of NMOS power MOSFET devices linear with TID up to 1 Mrad, independent of dose rate.
- For $V_{GS} \neq 0$ GIF samples, ΔV_T versus TID trends consistent with the TCAD results for various charge-centroid locations and acceptor-type interface traps
- For LINAC samples, however, the ΔV_T magnitudes were the same (up to 500 krad TID) irrespective of gate bias during exposure and require further verification/assessment
- GIF $V_{GS}=0V$ sample exhibited strong V_T rebound for TID > 200 krad. Post-TID I_D - V_{GS} characterization reveals formation of acceptor-type interface traps and formation of negative bulk oxide charge.

- [1] Lauenstein, J.-M., et al, IEEE Nuc. & Space Rad. Effects Conf. (NSREC) Data Workshop, San Francisco, W38 (2013).
- [2] Winokur, P. S., et al, IEEE Trans. Nuc. Sci. NS-30, pp. 4326 (1983).
- [3] Fleetwood, D. M., et al, IEEE Trans. Nuc. Sci. NS-35, pp. 1497 (1988).
- [4] McWhorter, P. J., et al, IEEE Trans. Nucl. Sci. NS-37, pp. 1682 (1990).
- [5] Heiman, F. P. and Warfield, G., IEEE Trans. Electron Devices, ED-12, pp. 167 (1965).
- [6] Lai, S. K. J. Appl. Phys., v 54, pp. 2540, (1983).
- [7] Burghard, R. A., and Gwyn, C. W., IEEE Trans. Nucl. Sci. NS-20, pp. 300 (1973).